Novel Helix-Constrained Nociceptin Derivatives Are Potent Agonists and Antagonists of ERK Phosphorylation and Thermal Analgesia in Mice

ARTICLE *in* JOURNAL OF MEDICINAL CHEMISTRY · NOVEMBER 2010

Impact Factor: 5.45 · DOI: 10.1021/jm101139f · Source: PubMed

9 AUTHORS, INCLUDING:

Timothy Adrian Hill
University of Queensland
40 PUBLICATIONS **691** CITATIONS
SEE PROFILE

Rink-Jan Lohman
University of Queensland
19 PUBLICATIONS **277** CITATIONS
SEE PROFILE

Huy Ngoc Hoang
University of Queensland
54 PUBLICATIONS **701** CITATIONS
SEE PROFILE

David Fairlie
University of Queensland
230 PUBLICATIONS **7,546** CITATIONS
SEE PROFILE

Journal of Medicinal Chemistry Article

J. Med. Chem. **XXXX,** *XXX,* 000–000 **A**
DOI: 10.1021/jm101139f

Novel Helix-Constrained Nociceptin Derivatives Are Potent Agonists and Antagonists of ERK Phosphorylation and Thermal Analgesia in Mice[†]

Rosemary S. Harrison, Gloria Ruiz-Gómez, Timothy A. Hill, Shiao Y. Chow, Nicholas E. Shepherd, Rink-Jan Lohman, Giovanni Abbenante, Huy N. Hoang, and David P. Fairlie*

Division of Chemistry and Structural Biology, Institute for Molecular Bioscience, The University of Queensland, Brisbane, Queensland 4072, Australia

Received September 3, 2010

The nociceptin opioid peptide receptor (NOP, NOR, ORL-1) is a GPCR that recognizes nociceptin, a 17-residue peptide hormone. Nociceptin regulates pain transmission, learning, memory, anxiety, locomotion, cardiovascular and respiratory stress, food intake, and immunity. Nociceptin was constrained using an optimized helix-inducing cyclization strategy to produce the most potent NOP agonist (EC_{50} = 40 pM) and antagonist (IC_{50} = 7.5 nM) known. Alpha helical structures were measured in water by CD and 2D ^{1}H NMR spectroscopy. Agonist and antagonist potencies, evaluated by ERK phosphorylation in mouse neuroblastoma cells natively expressing NOR, increased 20-fold and 5-fold, respectively, over nociceptin. Helix-constrained peptides with key amino acid substitutions had much higher in vitro activity, serum stability, and thermal analgesic activity in mice, without cytotoxicity. The most potent agonist increased hot plate contact time from seconds up to 60 min; the antagonist prevented this effect. Such helix-constrained peptides may be valuable physiological probes and therapeutics for treating some forms of pain.

Introduction

Different forms of pain place significant health, economic, and lifestyle burdens on our aging communities, with escalating costs to society in pain management, disability payments, and reduced work productivity. Most of the limited treatments available have side effects or risks of addiction, and there are significant unmet needs for new therapeutics. Nociceptin (or orphanin FQ) is a 17-residue peptide (FGGFTGARKSARKLANQ) that binds the opioid-receptor-like-1 (ORL) receptor,[1] also called nociceptin/orphanin FQ peptide receptor, NOP receptor or NOR. NOR is a GPCR[a] with high sequence homology to other opioid receptors but with a different profile in pain transmission.[2−5] Nociceptin and NOR are widely distributed in the brain, central and peripheral nervous systems, and respiratory, cardiovascular, and immune systems.[6] They have been implicated in pain regulation, learning and memory, food intake, anxiety, and stress.[2−5] NOR has also been identified in mouse splenic leukocytes[7] and human immune tissues,[8,9] although immune functions remain ill-defined.[7,10,11] Recent reviews highlight growing interest in the therapeutic potential of NOR,[2−5,7] supported by gene knockdown/out studies and by diverse properties reported for selective agonists and antagonists in vitro and in vivo.[2−5,7]

Although few clinical trials have been conducted for selective NOR ligands, there are strong indications that both agonists and antagonists (even peptides) could be valuable for treating different types of acute and chronic pain. Agonists are indicated for antinociception/analgesia, neuropathic pain, hypertension, congestive heart failure, cough, dysmenorrhea, anorexia, urinary incontinence, anxiety, and alcohol and drug addiction,[2−5] while antagonists are indicated for treating some forms of acute and chronic pain, Parkinson's disease, cognition impairment, depression, and obesity.[3−5,7,12−16] The route of administration (peripheral or spinal/intrathecal) is important in determining agonist function,[17−20] with direct centrally administered NOR agonists resulting in hyperalgaesia.[17,21] Local peripheral administration of NOR compounds may be best for studying sensory (rather than neuropathic or chronic) nociception in simple analgesia assays, such as the hot plate paw-withdrawal latency or tail flick,[19,22] which does not require invasive experimental procedures or lead to results that are difficult to interpret.

Nociceptin(1−17) is composed of an N-terminal "message" tetrapeptide FGGF, that activates the receptor NOR, linked to a C-terminal "address" domain nociceptin(7−17), that provides high affinity and selectivity for the receptor, most likely through interaction of its basic amino acids with the acidic second extracellular loop of NOR.[1] Inhibition of cAMP

[†]All NMR data and derived three-dimensional structures for compounds **7**, **8**, and **11** have been deposited in the Biological Magnetic Resonance Bank [BMRB accession numbers: 320qis8 (**7**), 3z0q0y7 (**8**), and 3z0q0y9 (**11**)].

*To whom correspondence should be addressed. Phone +61-733462989. Fax: +61-733462990. E-mail: d.fairlie@imb.uq.edu.au.

[a] Abbreviations: Aib, α-aminoisobutyric acid; ANOVA, analysis of variance; BOP, benzotriazole-1-yloxytris(dimethylamino)phosphonium hexafluorophosphate; BzlGly, *N*-benzyl glycine; cAMP, cyclic adenosine monophosphate; CHO, Chinese hamster ovary; CD, circular dichroism; DCM, dichloromethane; DIPEA, *N*,*N*-diisopropylethylamine; DMEM, Dulbecco's modified Eagle medium; DSD, sodium dodecyl sulfate; ED, effective dose for in vivo efficacy; ERK, extracellular signal-regulated kinases; pERK, phosphorylated ERK; F(4-F) or Phe(4-F), 4-fluorophenylalanine; Phe(4-NO_2), 4-nitrophenylalanine; FBS, fetal bovine serum; GPCR, G-protein-coupled receptor; GTP, Guanosine-5′-triphosphate; PBS, phosphate buffered saline; PTX, pertussis toxin; PULCON, pulse length based concentration determination; RP-HPLC, reversed phase high performance liquid chromatography; rmsd, root-mean-square deviation; TFE, 2,2,2-trifluoroethanol.

Table 1. Agonist Activity for Acyclic (**1**−**6**) and Cyclic (**7**−**11**) Nociceptin Analogues Measured by pERK

Compound	Sequence	-log EC_{50} ± SEM	EC_{50} (nM)	E_{max} (%)
	Message-Hinge[a] domain Address domain			
1	H-FGGFTGARKSARKLANQ-OH	7.94 ± 0.16	11	90 ± 7
2	H-FGGFTGARKSARKLANQ-NH_2	7.89 ± 0.09	13	103 ± 6
3	H-FGGFTGARKSARK-NH_2	7.94 ± 0.14	11	90 ± 8
4	H-FGGF(4-F)TGARKSARKLKNQ-NH_2	9.44 ± 0.12	0.36	108 ± 9
5	H-FGGFTGK(Ac)RKSNRKK(Ac)ANQN-NH_2	6.45 ± 0.08	360	99 ± 8
6	H-FGGFTGARKSARKAANQA-NH_2	8.42 ± 0.15	4	93 ± 7
7[b]	H-FGGFT[KARKD][KRKLD]-NH_2	8.51 ± 0.14	3	96 ± 8
8[b]	H-FGGFTG[KRKSD]RK[KANQD]-NH_2	9.22 ± 0.08	0.61	94 ± 3
9[b]	H-FGGFTG[KRK[KD]RKD]-NH_2	7.86 ± 0.08	14	92 ± 5
10[b]	H-FGGFTG[KRKSD]RK-NH_2	7.52 ± 0.18	30	80 ± 15
11[b]	H-FGGF(4-F)TG[KRKSD]RK[KKNQD]-NH_2	10.40 ± 0.11	0.04	101 ± 6

[a] The hinge region of the nociceptin native sequence involves Thr5Gly6 residues. [b] Square brackets denote cyclic pentapeptide components formed by (i, $i+4$)-lactam bridges between lysine and aspartate side chains.

reveals that ligand potency for NOR depends upon residues Phe1, Gly2, Phe4, and Arg8,[3] as well as C-terminal amidation.[23] Substituting *N*-benzyl glycine (BzlGly) for Phe1 repositions the benzyl substituent at the N-terminus, leading to full antagonism but with low affinity and potency.[24] Potency was increased over native nociceptin by Arg14 and Lys15 substitutions[21,25,26] or by introducing an electron-withdrawing group *para* in the aromatic side chain of Phe4, such as Phe(4-F)4 and Phe(4-NO_2)4, as shown in mouse vas deferens, mouse forebrain membranes, and forskolin stimulated cAMP in CHO_{hOP4} cells.[27]

Nociceptin has negligible helical structure in water, but CD and NMR spectroscopic studies have shown some propensity for α-helicity between residues 4 and 17 in aqueous sodium dodecylsulphate (SDS) micelles, a solvent that simulates a membrane environment to some extent.[28] Introduction of Aib at positions 7 and 11 in [Phe(4-F)4,Aib7,Aib11,Arg14,Lys15]-nociceptin(1−17)-NH_2 to help stabilize helicity reportedly resulted in the most potent agonist and antagonist known.[29] Peptides constrained by disulfide bonds at positions $i \rightarrow i+11$ or $i \rightarrow i+7$ or $i \rightarrow i+4$ showed the highest affinity, especially cyclo-[Cys10,Cys14]-nociceptin(1−14)-NH_2 (IC_{50} = 4.4 nM).[30] A small library of nociceptin(1−13)-NH_2 peptides constrained by Asp(6) → Lys(10) or D-Asp(7) → Lys(10) lactam bridges show up to 7-fold higher affinity and ^{35}S-GTPγS activation than when uncyclized and 2-fold over nociceptin-(1−13)-NH_2.[31]

Our work on helix-constraining strategies in short peptides[32−35] suggested that nociceptin peptides to date might not have been optimally α-helical in the address domain. Analogues with higher α-helicity in the address domain might exhibit enhanced agonist or antagonist activity, as well as higher stability in serum that can bring greater utility in vivo. To test this hypothesis, specific new lactam bridges have been incorporated at key positions within nociceptin(1−17)-NH_2 and analogues. CD and NMR spectroscopy have been used to investigate structures of new compounds, and an ERK assay using native cell lines was developed to assess activation of native NOR. In addition, serum stability, hemolytic activity, and in vivo analgesic activity have been examined for selected potent helix-constrained nociceptin analogues. The resulting compounds are the most potent NOR agonists and antagonists reported to date, establishing that strategic introduction of specific α-helix-inducing constraints improves potency and serum stability, with utility demonstrated in vivo in a mouse model of thermal nociception.

Design of Nociceptin Mimetics. Six known linear peptide analogues of FGGFTGARKSARKLANQ were chosen as comparators for this study (**1**−**6**, Table 1). They included two simple versions of nociceptin(1−17) with a C-terminal acid (**1**) or amide (**2**) but free N-terminus, a truncated analogue nociceptin(1−13) (**3**), an analogue (**4**) with substitutions at positions 4 (Phe(4-F)) and 15 (Lys), an analogue (**5**) with substitutions at positions 7 and 14 (Lys(Ac)) and 11 (Asn), an additional C-terminal residue (Asn), and a compound (**6**) with a change at position 14 (Ala) as well as an additional C-terminal residue (Ala). Five novel derivatives of these peptides were devised with cyclic pentapeptide components (**7**−**11**, Table 1) to probe the effect of helix induction on agonist potency. These cyclic components were created through side chain to side chain lactam bridges positioned strategically either back-to-back (**7**), separated by two amino acids (**8**, **11**), or overlapping (**9**), and in one case (**10**) only one cyclic constraint was used (Figure 1). We expected to be able to convert the resulting cyclic helical agonists (Table 1) to antagonists **15**−**20** by removing the N-terminal message domain or by replacing the N-terminal phenylalanine (Phe1) with *N*-benzylglycine (BzlGly1) (Table 2). Higher potency was expected over linear peptides through creation of these helix-constrained cyclic pentapeptide modules within the address domain, together with key substitutions also reported in message (Phe4Phe(4-F)) and address (Ala15Lys) domains of unconstrained linear analogues of nociceptin.[21,24−27]

Helical Structure of Nociceptin(1−17)-NH_2 Analogues in Water. The structures of all nociceptin peptides in 10 mM phosphate buffer (pH 7.4) at 22 °C were investigated by CD spectroscopy. All unconstrained peptides (**1**−**6** and **12**−**14**) showed minimal helicity (< 6%) in this buffer, as calculated from molar ellipticity at λ = 222 nm, the addition of the helix-promoting 2,2,2-trifluoroethanol (TFE) only marginally increasing helicity (Figure 2, Table S1).[36] By comparison, two lactam bridges to create helical cyclic peptide templates within the sequences did induce appreciable helicity (32−71%), limited by the presence at the N-terminus of amino acids FGGFTG not in the helix-constrained region and other amino acids not expected to be helical, as they have little propensity to occur

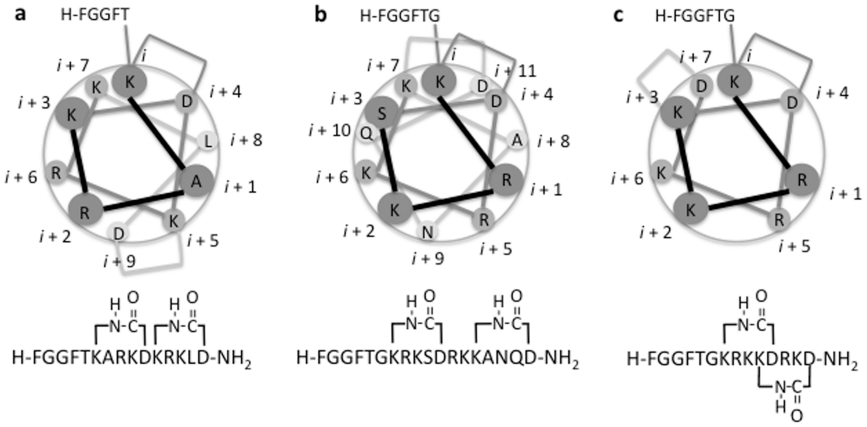

Figure 1. Helical wheel diagrams for different types of designed cyclic mimetics of nociceptin. Three prospective cyclization strategies show the relative bridge positions (with two lactam-bridged cyclic pentapeptide regions within the sequence) and conservation of Phe1, Gly2, Phe4, Thr5, Arg8, Leu14 (only a), and Ala15 (only b).

Table 2. Antagonist Activity for Nociceptin Analogues Measured by pERK

Compound	Sequence	-log IC_{50} ± SEM	IC_{50} (nM)
	Message-Hinge[a] domain Address domain		
12	BzlGlyGGFTG ARKSARKLKNQ-NH_2	7.40 ± 0.11	39
13	BzlGlyGGF(4-F)TG ARKSARKLKNQ-NH_2	7.49 ± 0.09	32
14	BzlGlyGGFTG ARKSARK-NH_2	6.22 ± 0.08	755
15[b]	BzlGlyGGFTG [KRKSD]RK[KKNQD]-NH_2	7.91 ± 0.10	12
16[b]	BzlGlyGGF(4-F)TG [KRKSD]RK[KKNQD]-NH_2	8.12 ± 0.11	7.5
17[b]	BzlGlyGGFT [KARKD][KRKLD]-NH_2	<7	IA[c]
18[b]	AcT [KARKD][KRKLD]-NH_2	<7	IA[c]
19[b]	Ac- [KRKSD]RK[KKNQD]-NH_2	<7	IA[c]
20[b]	H-TG [KRKSD]RK[KKNQD]-NH_2	<7	IA[c]

[a] The hinge region of the nociceptin native sequence involves Thr5Gly6 residues. [b] Square brackets denote cyclic pentapeptide components formed by (i, $i + 4$)-lactam bridges between lysine and aspartate side chains. [c] Inactive at maximum concentration tested, 100 nM.

in α-helices in proteins. To determine whether exocyclic regions were the cause of low overall helicity, compound **19** without the N-terminal message was investigated further. This 12-residue peptide features eight residues (K, R, Q) known to favor α-helicity in proteins and was 60% helical in phosphate buffer by CD spectral analysis (Table S1), close to the proportion (2/3) of such amino acids known to favor helicity in proteins. The serine residue is conserved in the sequence of many of these peptides and is a known helix breaker. In summary, the CD spectra suggested that compounds **7**, **8**, **9**, **11** and **15**−**20** were significantly α-helical in aqueous phosphate buffer (Figure 2, Table S1).

Solution structures were investigated by 1D and 2D ^{1}H NMR spectra in 90% H_2O/10% D_2O at 288−298 K, calculated using the program XPLOR and deposited in a relevant database for compounds **7** (BMRB, 320qis8), **8** (BMRB, 3z0q0y7), and **11** (BMRB, 3z0q0z0). The three-dimensional structures were very similar for **7** and **8** (Figure 3), with high α-helicity in the constrained cyclic regions that form three to four α-helical turns and a nonhelical turn for message residues (FGGFTG) at the N-terminus. The back-to-back arrangement of cyclic pentapeptides in compound **7** gave a backbone pairwise rmsd of 0.31 Å for the 20 lowest energy structures (Figure 3), indicating high structural convergence. Compounds **8** and **11**, with the same helical address domain, had a higher rmsd for their bicyclic components separated by two residues (**8**, rmsd [K7-D18] 0.75 Å; **11**, rmsd [K7-D18] 0.68 Å), suggesting more flexibility in these structures. Superimposition of the helical components of these structures on idealized (i.e., $\phi = -57°$, $\psi = -47°$) α-helical peptides of 10- and 12-residues gave average pairwise backbone rmsd of 0.18 Å (**7**), 0.35 Å (**8**), and 0.31 Å (**11**). Unlike **7**, helix-constrained cyclic regions in **8** and **11** contain Ser and Asn residues that are not helix favoring in proteins. Greater flexibility for the unconstrained message domain (FGGFTG) may enable access to a turnlike conformation, likely required for recognition and activation of the GPCR.[37] Compound **8** in particular displayed some turn structure at the N-terminus, suggested by hydrogen bonding into this region from residues K7 and R8 and by strong $d_{\alpha N(i,i+2)}$ and $d_{\alpha N(i,i+3)}$ but missing $d_{\alpha N(i,i+4)}$, NOEs (Figure S10). This may be a clue for design of N-terminal turn peptidomimetics attached to the helical address domain.

Agonist Activity. Intracellular calcium release, cAMP stimulation, and ERK1/2 phosphorylation were each investigated for examining signaling by nociceptin(1−17)-OH (**1**) in three different untransfected cell lines: human monocytes U937, human neuroblastoma SH-SY5Y cells, mouse neuroblastoma Neuro-2a cells. Nociceptin(1−17)-OH (1 μM) did not induce intracellular calcium release in any of these native cell lines,

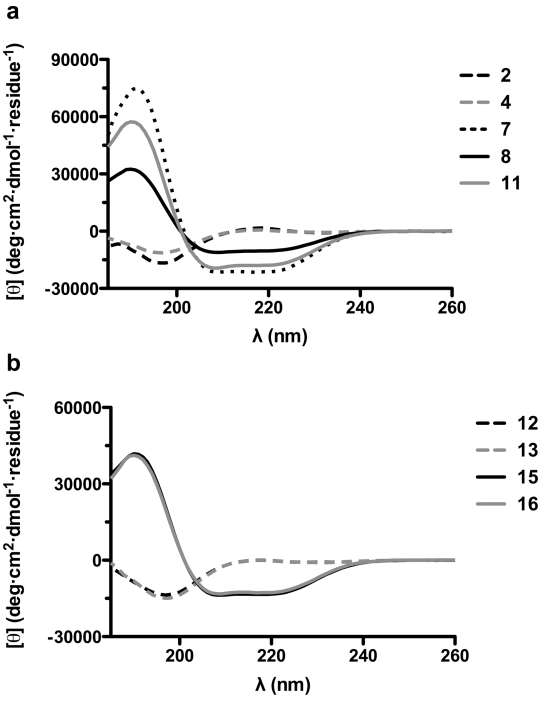

Figure 2. CD spectra for different agonist and antagonist nociceptin mimetics: (a) unconstrained agonists **2** (2 black dashes) and **4** (2 grey dashes) and the helix-constrained agonist nociceptin mimetics **7** (3 black dots), **8** (black line), and **11** (grey line); (b) unconstrained antagonists **12** (2 black dashes) and **13** (2 grey dashes) and constrained antagonists **15** (black line) and **16** (grey line).

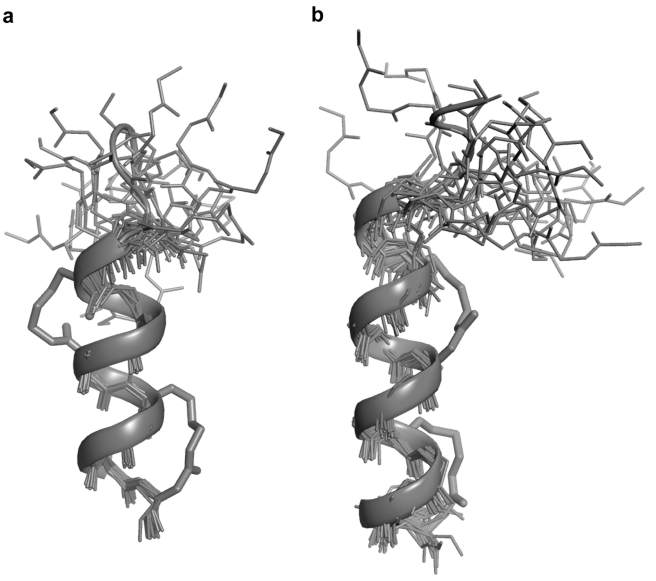

Figure 3. NMR-derived solution structures for helix-constrained compounds **7** and **8**. The 20 lowest energy conformations are shown for (a) **7** (rmsd = 0.31 Å (K6-D15)) and (b) **8** (rmsd = 0.75 Å (K7-D18)). Lactam bridges are displayed as sticks, and C-terminus is at the bottom for each peptide.

even after priming[38] with carbacol. Nociceptin did not inhibit cAMP in U937 cells but did inhibit cAMP in Neuro-2a and SH-SY5Y cells though not through PTX-sensitive G proteins. However, nociceptin did induce ERK phosphorylation (pERK2) in U937 and Neuro-2a cells, while SH-SY5Y cells had a constitutively high background pERK, making it difficult to detect pERK arising from nociceptin(1−17)-OH treatment. Therefore, we report data herein for pERK2 detection in Neuro-2a cells, measured using an antibody-based AlphaScreen Surefire kit. While this manuscript was in preparation, nociceptin was reported to signal through ERK-1/2 in rat neurons.[39]

Eleven compounds were tested for agonist activity over a range of concentrations (Table 1, Figure 4). Wild type nociceptin(1−17)-OH (**1**) was equipotent (EC_{50} = 11 nM) with amidated analogues **2** and **3** (Figure 4a). Modifications Phe4Phe(4-F) and Ala15Lys provided 30-fold enhanced agonist potency (EC_{50} = 360 pM, log EC_{50} = −9.44 ± 0.12, $p \leq 0.001$). The three different cyclization strategies used to induce helicity in the address domain significantly affected the extent of NOR activation, as measured by ERK phosphorylation (Figure 4b). For example, compound **7** featuring two back-to-back lactam bridges showed improved activity over the unconstrained analogue **2** (EC_{50} = 3 nM, pEC_{50} = 8.51 ± 0.14, $p \leq 0.05$). Spacing the two bridges apart as in **8** further improved agonist potency (EC_{50} = 610 pM, pEC_{50} = 9.22 ± 0.08). On the other hand, when the two lactam bridges overlapped as in **9**, there was no improvement in agonist potency over **2**.

Since **8**, with two spaced cyclic pentapeptide constraints, was the most effective agonist scaffold, it was further modified to compound **11**, featuring two amino acid substitutions Phe4Phe(4-F) and Ala15Lys shown by us (Table 1) and others to improve agonist potency. These substitutions significantly increased agonist activity (Figure 4c), affording the most potent superagonist **11** (EC_{50} = 40 pM), relative to **8** (EC_{50} = 610 pM) and its unconstrained analogue **4** (EC_{50} = 360 pM; $p \leq 0.001$) (Table 1). To establish that the increased agonist potency for **8** and **11** was not due to simple replacement of amino acids, we examined compounds **5** and **6** in which amino acids 7, 11, and 14 and an extra residue 18 were replaced by either alanine or Lys(Ac)/Asn (compounds **5** and **6**). The lysine side chain amine was charge neutralized with an acetyl group to more effectively mimic the lactam bridging residues. Asparagine rather than aspartic acid was used to maintain the length of the side chain while removing the negative charge of the carboxylic acid moiety. Alanine replacements in **6** moderately increased agonist activity (although $p \geq 0.05$), and replacement with Lys(Ac)/Asn in **5** substantially decreased agonist potency (EC_{50} = 360 nM, $p \leq 0.001$, Figure 4c). Thus, changes to the amino acid sequence if anything hindered NOR binding rather than enhanced agonist activity, so we confidently attribute the potency increases in **8** and **11** to the effect of helix-inducing lactam bridges. Just one cyclic pentapeptide constraint (**10**, Figure 4d), equivalent to truncating **8** to residues 1−13, resulted in a lower fractional α-helicity (10%) and the lowest agonist potency. We also compared structural and biological properties of two previously reported analogues containing D-Asp in their sequence.[31] Constrained peptide H-cyclo-(7,11)-FGGFTG-[dRKSK]RK-NH_2 was inactive, whereas analogue H-cyclo-(7,10)-FGGFTG[dRKK]ARK-NH_2[31] had EC_{50} = 18 nM in our pERK assay. Our data suggest that both compounds have similar structures but no α-helicity (Table S1).

Antagonist Activity. Compound **12** is a known NOR antagonist and behaves as such in our ERK assay (IC_{50} = 39 nM, pIC_{50} = 7.40 ± 0.11, Table 2). Replacing Phe4 by *p*-fluorophenylalanine (**13**) did not affect antagonist potency, even though it significantly enhanced agonist potency of nociceptin analogues. This was unexpected as *para*-halogenation at position 4 is known to improve binding affinity, previously increasing antagonist potency 11-fold in vivo

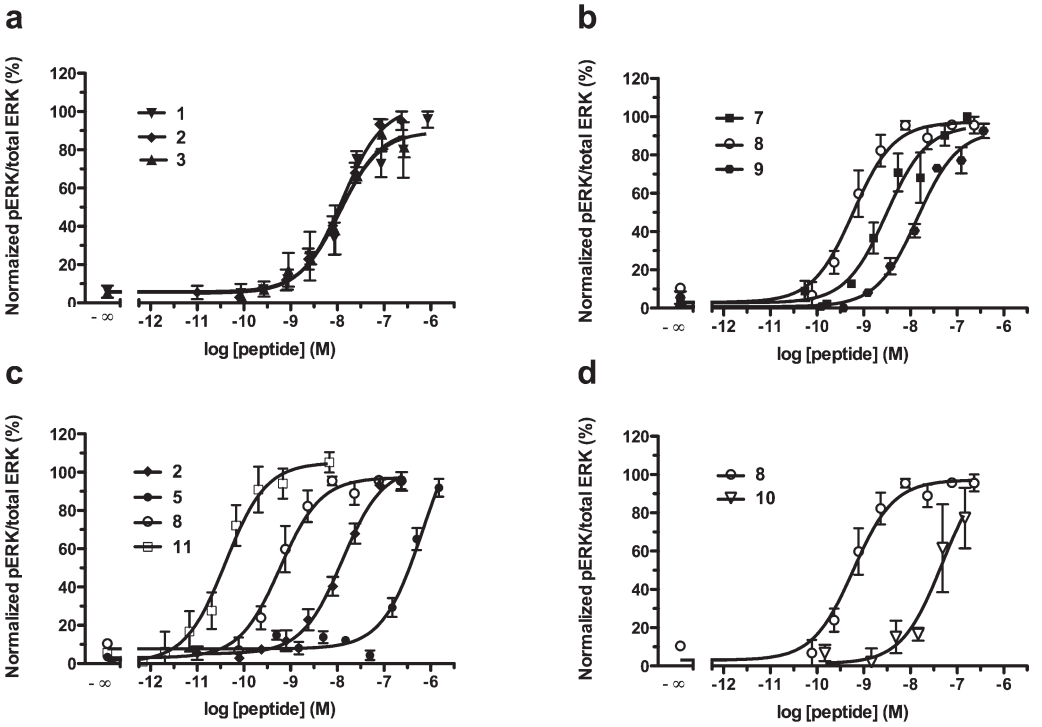

Figure 4. pERK concentration-response profiles for different agonists: (a) compounds **1** (▼), **2** (◆), and **3** (▲); (b) compounds **7** (■), **8** (○), and **9** (●); (c) compound **11** (□), **8** (○), and **5** (●) vs **2** (◆); (d) Compounds **8** (◆) vs **10** (▽). EC_{50} values for all compounds are reported in Table 1. All data are normalized to PBS control (0%) and 1 μM compound **1** (100%). All data points represent $n \geq 3$.

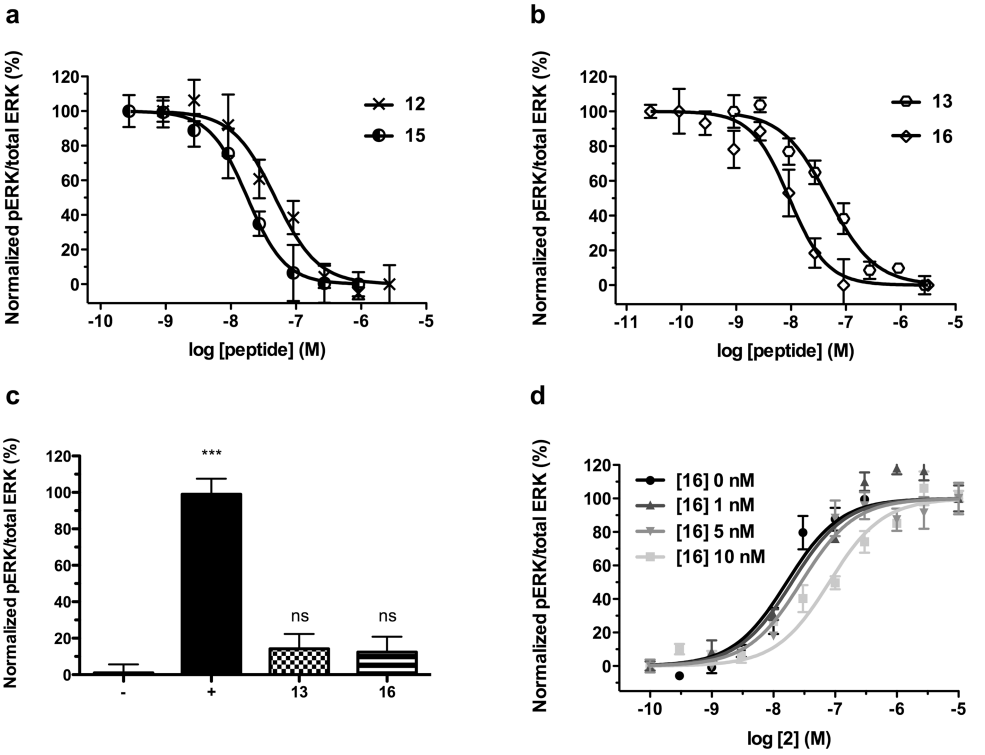

Figure 5. pERK concentration-response profiles for antagonist compounds: (a) **12** (×) vs **15** (◐); (b) **13** (○) vs **16** (◇). IC_{50} values are in Table 2. All data are normalized to PBS control (0%) and 100 nM **2** (100%). (c) pERK agonist residual activity of **13** and **16** at 1 μM concentration. Data are normalized to PBS control (0%) and 1 μM compound **2** (100%). Data have been analyzed using one way ANOVA. (d) Nociceptin-induced ERK phosphorylation inhibited by the helix-constrained peptide **16**. Concentration-response curves show that a higher concentration of nociceptin(1−17)-NH_2 is needed to produce the same effect in the presence of compound **16**. Statistical analysis ($p \leq 0.001$) was done using the *t* test. All data points represent $n \geq 3$. For illustration purposes only, the Hill slope was set to 1.0.

using electrically stimulated pig ileum.[40] However, NOR antagonist activity has not been reported via pERK signaling before and observations from different assays may not be directly comparable. Interestingly, removing the C-terminal

tetrapeptide sequence (LKNQ) from **12** reduced antagonist potency ~20 fold (**14**, Table 2), suggesting that these residues significantly contribute to antagonist activity, although not contributing greatly to agonist potency.[41]

When antagonists **12** and **13** were converted to helix-constrained analogues **15** and **16**, respectively, there was a 3- to 4-fold enhancement in antagonist potency (Table 2, Figure 5a,b). This enhancement due to helix constraints is much less than 20-fold noted for agonists above. On the basis of alanine mutants in the agonists (discussed above), we are confident that the enhanced antagonist potency is due to induction of helical structure in **15** and **16** rather than substitution of residues at positions 7, 11, 14, and 18. Shifting the spaced lactam bridges (K7 → D11, K14 → D18) in **15** and **16** to different positions (K6 → D10, K11 → D15) in **17** eliminated antagonist activity (up to 3 μM). This loss in activity may be due to (i) removal of G6 in the hinge (Thr5Gly6Ala7) between the message and address domains[42,43] or (ii) steric clashes between side chain bridges and receptor residues or (iii) removal of the KNQ N-terminus. Removing the C-terminal message domain (**18**−**20**) surprisingly abolished antagonist activity instead of competing with agonist binding to NOR. We believe that the BzlGly substituent at position 1 in these antagonists binds in a different location in NOR than does the phenylalanine in nociceptin and agonists, and thus, the helical region alone cannot antagonize nociceptin binding and function. There is some support for this assertion for **12**, [BzlGly1]nociceptin(1−17)-NH_2.[40,44]

Compounds **13** and **16** were also assessed for residual agonist activity, the aromatic group Phe(4-F) at the fourth position potentially contributing agonist activity despite the presence of BzlGly at position 1.[40] At 1 μM, neither compound showed agonist activity (Figure 5c). Specificity of our most potent agonist (**11**) was also investigated by pretreating cells with NOR antagonist **14** (1.5 μM) and significantly reduced the potency of increasing concentrations of added **11** (EC_{50} of 40 pM to 1 nM, $p \leq 0.001$; Figure S1, Table 1), suggesting that pERK agonist activity of **11** is mediated through NOR.

A competition experiment was conducted for the most potent antagonist, H-cyclo-(7,11;14,18)-BzlGGGF(4-F)TG[KRKSD]RK[KKNQD]-NH_2 (**16**), versus nociceptin(1−17)-NH_2 (**2**) to investigate the possibility of similar binding sites. Concentration-response curves (Figure 5d) for nociceptin-(1−17)-NH_2 alone and with antagonist (at 10, 5, and 1 nM) demonstrated that the fractional receptor occupancy by nociceptin(1−17)-NH_2 was lower in the presence of antagonist **16** than in its absence. Thus, higher concentrations of agonist were needed to produce the same maximal effect, suggesting that **16** is a reversible competitive antagonist with nociceptin-(1−17)-NH_2 for the same receptor. Consistent with this assertion, the Schild plot analysis has shown a slope of 1.0 and a pA_2 of 8.71 (2 nM) (Figure S2).

Stability and Cell Toxicity of Helix-Constrained vs Unconstrained Peptides. Compound **8** had a much longer half-life in normal human serum ($t_{1/2}$ > 6 h) than native nociceptin (compound **1**, $t_{1/2}$ 1 h) (Figure S3a). Neither cyclic peptides **8** and **11** nor the unconstrained nociceptin(1−17)-OH (**1**) had any hemolytic activity (Figure S3b).

Antinociceptive Response in Mice. In vivo activities were compared for helix-constrained peptide **11** versus unconstrained peptides **2** and **4**, following administration by intraplantar injection to C57BL/6 mice by monitoring front paw withdrawal response latencies to hot plate contact. Sham animals demonstrated a significantly reduced paw withdrawal latency following saline administration, suggesting some heightened thermal sensitivity following injection alone. Nociceptin (**2**) prevented this in the short term (Figure 6a), producing a dose-dependent increase in the thermal antinociceptive threshold, peaking at 400 pmol with ED_{50} = 184 pmol, similar to that reported in a different in vivo assay.[20] There was no response to nociceptin (**2**) after 5 min, suggesting rapid metabolism. The more potent linear peptide agonist (**4**) produced a comparable dose-dependent increase in thermal nociceptive threshold (ED_{50} = 161 pmol), with increased withdrawal latencies observed at 5 min but not at 15 min. This suggests that agonist **4** is more stable in vivo with only slightly greater potency than native nociceptin (**2**).

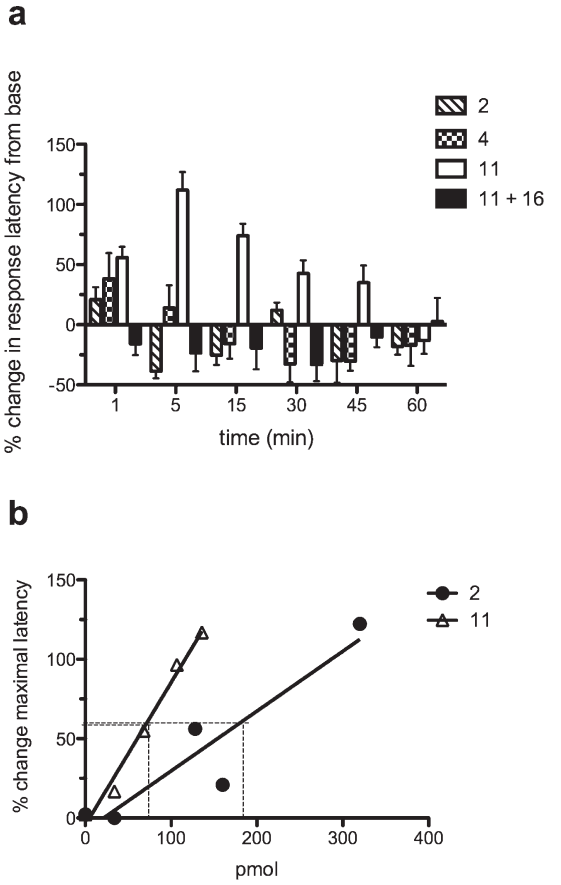

Figure 6. Nociceptive activity of helix-constrained peptides. (a) Front-paw withdrawal latency in response to 200 pmol **2** (~ED_{50}) on a hot plate (53 °C) after various times. Data show maximal increased thermal nociceptive threshold response, and duration of response is greater (up to 60 min) in animals treated with helix-constrained **11** than either **2** or **4** (< 5 min). Antagonist **16** (200 nmol) ameliorated changes in withdrawal latency induced by **11** (200 pmol) when coadministered. (b) Dose-response curves indicate that **11** (ED_{50} = 70 pmol) is more potent than **2** (ED_{50} = 184 pmol).

Helix-constrained agonist **11** produced a much more robust dose-dependent increase in withdrawal latency, lasting up to 60 min following administration (rep-mes ANOVA $p < 0.05$). Maximal responses to **2** and **11** were no different (~120% change increase in withdrawal latency, Figure 6b), but the ED_{50} of **11** (70 pmol) was substantially lower than for **2**. Thus, helix-constrained peptide **11** was significantly more potent than unconstrained peptides as an antinociceptive agent in vivo. When agonist **11** was coadministered (at ED_{100} = 200 pmol) with helical antagonist **16** (200 nmol), the increased paw withdrawal latency produced by agonist **11** alone was abolished, confirming that helix-constrained peptide **16** is a

potent antagonist of agonist **11** in vivo (Figure 6a) most likely through acting on NOR in vivo.

Conclusions

Induction of α-helicity in nociceptin clearly enhanced agonist potency by up to 20-fold at the NOP receptor NOR, with optimal activity provided by incorporating known amino acid substitutions together with optimal helix-inducing constraints. Using strategic positioning of helix-inducing constraints, we have developed the most potent NOR superagonist (**11**) and antagonist (**16**) known to date, the antagonist being a reversible and competitive ligand with nociceptin. The helix-constrained compounds were not hemolytic and had superior serum stability over their unconstrained peptide analogues, making this series of compounds useful both in vitro and in vivo. Compound **11** was much more efficacious in thermal antinociception than nociceptin(1−17)-NH_2 (**2**) at the same dose, an effect that was significantly longer lasting than for nociceptin (**2**) or its analogue (**4**). It may be possible to further use the α-helix stabilized address domain of **8** and **11** as a template for supporting nonpeptidic fragments that can more effectively bind to the receptor than the message domain of antagonist **16**. This helix-constraining strategy may be a more valuable approach to new molecular probes, and possibly therapeutics for the treatment of pain, than previously realized. These results also exemplify a potentially generic strategy for preorganizing short peptides in protein-binding helical conformations to enhance induction or blockade of GPCRs and protein−protein interactions,[37,45] which mediate many important biological and physiological processes.

Experimental Methods

Methods for cell assays for cAMP, intracellular calcium release, ERK phosphorylation, as well as peptide synthesis, HPLC procedures, and NMR structure calculations are detailed in Supporting Information.

Peptide Synthesis. Peptides were synthesized by standard Fmoc chemistry methods described elsewhere.[32,33] The phenyl isopropyl ester of aspartic acid and methyltrityl group of lysine were removed from the peptide-resin with 3% TFA in dichloromethane (DCM) (5 × 2 min). Cyclization was effected on-resin using benzotriazole-1-yloxytris(dimethylamino)phosphonium hexafluorophosphate (BOP) and *N*,*N*-diisopropylethylamine (DIPEA) as base. The procedure was repeated for multiple cyclizations. Crude peptides were purified by RP-HPLC (solvent A = 0.1% TFA in H_2O, solvent B = 0.1% TFA, 10% H_2O in acetonitrile; gradient of 0% B to 40% B over 40 min; analytical RP-HPLC t_R obtained using a Phenomenex Luna C18 5 μm column, 250 mm × 4.60 mm, λ = 214 nm). Compounds were >98% pure by analytical HPLC. Retention times and mass spectral data are listed in Table S2.

Circular Dichroism. Measurements were made for compounds (50−200 μM, 500 μL) in 10 mM phosphate buffer (pH 7.4) in a 0.1 cm quartz cell with a Jasco J-710 spectropolarimeter (λ 185−260 nm) calibrated with (1*S*)-(+)-10-camphorsulfonic acid. Peptide concentration was determined by NMR (pulse length based concentration determination, PULCON),[46] % helicity calculated from molar ellipticities at λ = 222 nm.[33]

Structure Calculations. 1D and 2D (TOCSY, NOESY, DQF-COSY) ^{1}H NMR spectra were recorded on a Bruker Avance 600 spectrometer with water suppression (WATERGATE) at 288−298 K for peptides (2−3 mg) dissolved in 600 μL of H_2O/D_2O (9:1) at pH 4.0−5.0.[47] Spectra were processed using Topspin (Bruker), and NOE intensities were collected manually. ^{1}H chemical shifts were referenced to DSS (δ 0.00 ppm) in water. $^3J_{NHC\alpha}$ coupling constants were measured from 1D ^{1}H NMR and DQF-COSY spectra. Distance restraints in solution structure calculations were derived from NOESY spectra (mixing time of 250−300 ms). Calculations were performed using XPLOR[48] with modifications to generate lactam bridges.[35] Final structures had no distance (>0.2 Å) or angle (>5°) violations and were deposited with all NMR data in Biological Magnetic Resonance Bank (BMRB: 320qis8 (**7**), 3z0q0y7 (**8**), 3z0q0z0 (**11**)).

NOR Activation. Neuro-2a cells were cultured in DMEM and 10% FBS supplemented with nonessential amino acids. Cells were placed in 12-well plates (NUNC, NY) and allowed to adhere for 24−36 h. Medium was removed and replaced with serum free media for 12−15 h prior to use. Initially, cells were challenged with compounds for increasing time periods, and 35 min was optimal to initiate pERK signaling. For agonist assays, cells were challenged with compounds for 35 min and incubated at 37 °C (5% CO_2). For antagonist assays, cells were preincubated with test compound for 15 min (37 °C, 5% CO_2) and then challenged with 100 nM nociceptin(1−17)-NH_2 for 35 min. pERK and total ERK concentrations were determined using the AlphaScreen Surefire assay, and the ratio of pERK to total ERK was normalized to PBS control (0%) and 1 μM nociceptin-(1−17)-OH (100%). Responses were analyzed using nonlinear regression (variable slope) (Prism5, GraphPad Software) and data presented as EC_{50} (agonists) or IC_{50} (antagonists).

Nociceptive Activity in Mice. Agonists **2**, **4**, and **11** were tested for dose-response activity on paw-withdrawal latency in a hot plate test. Briefly, male C57BL/6 mice (25−30 g) were acclimatized to the experimental room for at least 30 min prior to testing. Mice were individually placed on an accredited thermal analgesiometer hot plate (Harvard Apparatus), heated to 53 ± 0.4 °C to obtain a baseline recording. Response times to any front paw withdrawal were measured, and licking or jumping behavior was recorded and deemed the nociceptive threshold. Mice were then injected with a peptide (**2**, **4**, or **11**, $n = 4-6$ per group; 0, 50, 100, 160, 200, 400, or 1000 pmol, intraplantar, 20 μL in sterile saline) into each front paw and immediately retested on the hot plate. Baseline controls were mice that received vehicle only. Similar procedures were used for antagonist testing, except both antagonist (**16**) (200 nmol) and agonist (**11**) (200 pmol) were coadministered. Each mouse was retested for withdrawal response at time points 5, 15, 30, 45, and 60 min after injection. Mice were not left on the hot plate for longer than 30 s, regardless of response, as prescribed by ethical agreement. Tests were video monitored for future reference. Data are expressed as a percentage change in withdrawal response time from baseline (0 pmol), mean ± SEM. Statistical analysis was performed using repeated measures using ANOVA with Bonferroni post-tests.

Acknowledgment. We thank Australian Research Council (ARC) for Grants DP0210330, DP0770936, and DP1093245 and National Health and Medical Research Council for Grant 511194. D.P.F. is supported by ARC Federation Fellowship FF668733, and G.R.-G. is supported by a postdoctoral fellowship from Ministerio de Educación y Ciencia (MEC) and Fundación Española para la Ciencia y la Tecnología (FECYT) (Spain). We thank Dr. Hanzal-Bayer and Prof. Mattick (University of Queensland, Australia) for PC12 and Neuro-2a cells.

Supporting Information Available: Experimental and analytical data (Table S2) for compounds **1**−**20** (>98% purity), NMR data including NOE summaries and refinement statistics for 20 lowest energy structures for **7** and **8** (Tables S3−S8, Figures 4−12), CD spectral data for **1**−**20** (Table S1), and assay data for determining agonist and antagonist potencies (Figure S1), hemolytic activity and serum stability (Figure S3), and nociception. This material is available free of charge via the Internet at http://pubs.acs.org.

References

(1) Meunier, J. C.; Mollereau, C.; Toll, L.; Suaudeau, C.; Moisand, C.; Alvinerie, P.; Butour, J. L.; Guillemot, J. C.; Ferrara, P.; Monsarrat, B.; Mazarguil, H.; Vassart, G.; Parmentier, M.; Costentin, J. Isolation and structure of the endogenous agonist of opioid receptor-like ORL1 receptor. *Nature* **1995**, *377*, 532–535.

(2) Chiou, L. C.; Liao, Y.-Y.; Fan, P. C.; Kuo, P.-H.; Wang, C.-H.; Riemer, C.; Prinssen, E. P Nociceptin/orphanin FQ peptide receptors: pharmacology and clinical implications. *Curr. Drug. Targets* **2007**, *8*, 117–135.

(3) Lambert, D. G. The nociceptin/orphanin FQ receptor: a target with broad therapeutic potential. *Nat. Rev.* **2008**, *7*, 694–710.

(4) Mustazza, C.; Bastanzio, G. Development of nociceptin receptor (NOP) agonists and antagonists. *Med. Res. Rev.* [Online early access]. DOI: 10.1002/med.20197. Published Online: Jan 22, 2010.

(5) Largent-Milnes, T. M.; Vanderah, T. W. Recently patented and promising ORL-1 ligands: where have we been and where are we going? *Expert Opin. Ther. Pat.* **2010**, *20*, 291–305.

(6) Mollereau, C.; Mouledous, L. Tissue distribution of the opioid receptor-like (ORL1) receptor. *Peptides* **2000**, *21*, 907–917.

(7) Halford, W. P.; Gebhardt, B. M.; Carr, D. J. Functional role and sequence analysis of a lymphocyte orphan opioid receptor. *J. Neuroimmunol.* **1995**, *59*, 91–101.

(8) Wick, M. J.; Minnerath, S. R.; Roy, S.; Ramakrishnan, S.; Loh, H. H. Expression of alternate forms of brain opioid "orphan" receptor mRNA in activated human peripheral blood lymphocytes and lymphocytic cell lines. *Mol. Brain Res.* **1995**, *32*, 342–347.

(9) Peluso, J.; LaForge, K. S.; Matthes, H. W.; Kreek, M. J.; Kieffer, B. L.; Gavériaux-Ruff, C. Distribution of nociceptin/orphanin FQ receptor transcript in human central nervous system and immune cells. *J. Neuroimmunol.* **1998**, *81*, 184–192.

(10) Peluso, J.; Gavériaux-Ruff, C.; Matthes, H. W.; Filliol, D.; Kieffer, B. L. Orphanin FQ/nociceptin binds to functionally coupled ORL1 receptors on human immune cell lines and alters peripheral blood mononuclear cell proliferation. *Brain Res. Bull.* **2001**, *54*, 655–660.

(11) Anton, B.; Leff, P.; Meissler, J. J.; Calva, J. C.; Acevedo, R.; Salazar, A.; Matus, M.; Flores, A.; Martinez, M.; Adler, M. W.; Gaughan, J. P.; Eisenstein, T. K. Nociceptin/orphanin FQ suppresses adaptive immune responses in vivo and at picomolar levels in vitro. *J. Neuroimmune Pharmacol.* **2010**, *5*, 143–154.

(12) Hu, E.; Calò, G.; Guerrini, R.; Ko, M. C. Long-lasting antinociceptive spinal effects in primates of the novel nociceptin/orphanin FQ receptor agonist UFP-112. *Pain* **2010**, *148*, 107–113.

(13) Klukovits, A.; Tekes, K.; Gündüz Çinar, Ö.; Benyhe, S.; Borsodi, A.; Deák, B. H.; Hajagos-Tóth, J.; Verli, J.; Falkay, G.; Gáspár, R. Nociceptin inhibits uterine contractions in term-pregnant rats by signaling through multiple pathways. *Biol. Reprod.* **2010**, *83*, 36–41.

(14) Murphy, N. P. The nociceptin/orphanin FQ system as a target for treating alcoholism. *CNS Neurol. Disord.: Drug Targets* **2010**, *9*, 87–93.

(15) Volta, M.; Marti, M.; McDonald, J.; Molinari, S.; Camarda, V.; Pelà, M.; Trapella, C.; Morari, M. Pharmacological profile and antiparkinsonian properties of the novel nociceptin/orphanin FQ receptor antagonist 1-[1-cyclooctylmethyl-5-(1-hydroxy-1-methyl-ethyl)-1,2,3,6-tetrahydro-pyridin-4-yl]-3-ethyl-1,3-dihydro-benzoimidazol-2-one (GF-4). *Peptides* **2010**, *31*, 1194–1204.

(16) Mabrouk, O, S; Marti, M.; Morari, M. Endogenous nociceptin/orphanin FQ (N/OFQ) contributes to haloperidol-induced changes of nigral amino acid transmission and parkinsonism: a combined microdialysis and behavioral study in naive and nociceptin/orphanin FQ receptor knockout mice. *Neuroscience* **2010**, *166*, 40–48.

(17) Mogil, J. S.; Pasternak, G. W. The molecular and behavioral pharmacology of the orphanin FQ/nociceptin peptide and receptor family. *Pharmacol. Rev.* **2001**, *53*, 381–415.

(18) Ko, M. C.; Naughton, N. N. Antinociceptive Effects of Nociceptin/Orphanin FQ Administered Intrathecally in Monkeys. *J. Pain* **2009**, *10*, 509–516.

(19) Reiss, D.; Wichmann, J.; Tekeshima, H.; Kieffer, B. L.; Ouagazzal, A. M. Effects of nociceptin/orphanin FQ receptor (NOP) agonist, Ro64-6198, on reactivity to acute pain in mice: comparison to morphine. *Eur. J. Pharmacol.* **2008**, *579*, 141–148.

(20) Sakurada, T.; Komatsu, T.; Moriyama, T.; Sasaki, M.; Sanai, K.; Orito, T.; Sakurada, C.; Sakurada, S. Effects of intraplantar injections of nociceptin and its N-terminal fragments on nociceptive and desensitized responses induced by capsaicin in mice. *Peptides* **2005**, *26*, 2505–2512.

(21) Calo, G.; Rizzi, A.; Rizzi, D.; Bigoni, R.; Guerrini, R.; Marzola, G.; Marti, M.; McDonald, J.; Morari, M.; Lambert, D. G.; Salvadori, S.; Regoli, D. [Nphe1,Arg14,Lys15]nociceptin-NH_2, a novel potent and selective antagonist of the nociceptin/orphanin FQ receptor. *Br. J. Pharmacol.* **2002**, *136*, 303–311.

(22) King, M. A.; Rossi, G. C.; Chang, A. H.; Williams, L.; Pasternak, G. W. Spinal analgesic activity of orphanin FQ/nociceptin and its fragments. *Neurosci. Lett.* **1997**, *223*, 113–116.

(23) Reinscheid, R. K.; Ardati, A.; Monsma, F. J., Jr.; Civelli, O. Structure−activity relationship studies on the novel neuropeptide orphanin FQ. *J. Biol. Chem.* **1996**, *271*, 14163–14168.

(24) Guerrini, R.; Salvadori, S.; Calo, G.; Bigoni, R.; Rizzi, D.; Regoli, D. Structure−activity relationship of [Nphe1]-NC-(1−13)-NH_2, a pure and selective nociceptin/orphanin FQ receptor antagonist. *J. Pept. Res.* **2001**, *57*, 215–222.

(25) Okada, K.; Sujaku, T.; Chuman, Y.; Nakashima, R.; Nose, T.; Costa, T.; Yamada, Y.; Yokoyama, M.; Nagahisa, A.; Shimohigashi, Y. Highly potent nociceptin analog containing the Arg-Lys triple repeat. *Biochem. Biophys. Res. Commun.* **2000**, *278*, 493–498.

(26) McDonald, J.; Calo, G.; Guerrini, R.; Lambert, D. G. UFP-101, a high affinity antagonist for the nociceptin/orphanin FQ receptor: radioligand and GTPgamma(35)S binding studies. *Naunyn Schmiedeberg's Arch. Pharmacol.* **2003**, *367*, 183–187.

(27) Guerrini, R.; Caló, G.; Bigoni, R.; Rizzi, D.; Rizzi, A.; Zucchini, M.; Varani, K.; Hashiba, E.; Lambert, D. G.; Toth, G.; Borea, P. A.; Salvadori, S.; Regoli, D. Structure−activity studies of the Phe(4) residue of nociceptin(1−13)-NH_2: identification of highly potent agonists of the nociceptin/orphanin FQ receptor. *J. Med. Chem.* **2001**, *44*, 3956–3964.

(28) Orsini, M. J.; Nesmelova, I.; Young, H. C.; Hargittai, B.; Beavers, M. P.; Liu, J.; Connolly, P. J.; Middleton, S. A.; Mayo, K. H. The nociceptin pharmacophore site for opioid receptor binding derived from the NMR structure and bioactivity relationships. *J. Biol. Chem.* **2005**, *280*, 8134–8142.

(29) Chang, M.; Peng, Y. L.; Dong, S. L.; Han, R. W.; Li, W.; Yang, D. J.; Chen, Q.; Wang, R. Structure−activity studies on different modifications of nociceptin/orphanin FQ: identification of highly potent agonists and antagonists of its receptor. *Regul. Pept.* **2005**, *130*, 116–122.

(30) Ambo, A.; Hamazaki, N.; Yamada, Y.; Nakata, E.; Sasaki, Y. Structure−activity studies on nociceptin analogues: ORL1 receptor binding and biological activity of cyclic disulfidecontaining analogues of nociceptin peptides. *J. Med. Chem.* **2001**, *44*, 4015–4018.

(31) Charoenchai, L.; Wang, H.; Wang, J. B.; Aldrich, J. V. High affinity conformationally constrained nociceptin/orphanin FQ-(1−13) amide analogues. *J. Med. Chem.* **2008**, *51*, 4385–4387.

(32) Shepherd, N. E.; Hoang, H. N.; Abbenante, G.; Fairlie, D. P. Single turn alpha helical peptides with exceptional stability in water. *J. Am. Chem. Soc.* **2005**, *127*, 2974–2983.

(33) Shepherd, N. E.; Abbenante, G.; Fairlie, D. P. Consecutive cyclic pentapeptide modules form short α-helices that are very stable to water and denaturants. *Angew. Chem., Int. Ed.* **2004**, *43*, 2687–2690.

(34) Shepherd, N. E.; Hoang, H. N.; Desai, V. S.; Letouze, E.; Young, P. R.; Fairlie., D. P. Modular alpha helical mimetics with antiviral activity against respiratory syncitial virus. *J. Am. Chem. Soc.* **2006**, *128*, 13284–13289.

(35) Harrison, R. S.; Shepherd, N. E.; Hoang, H. N.; Ruiz-Gómez, G.; Hill, T. A.; Driver, R. W.; Desai, V. S.; Young, P. R.; Abbenante, G.; Fairlie, D. P. Downsizing human, bacterial, and viral proteins to short water-stable alpha helices that maintain biological potency. *Proc. Natl. Acad. Sci. U.S.A.* **2010**, *107*, 11686–11691.

(36) Klaudel, L.; Legowska, A.; Brzozowski, K.; Silberring, J.; Wojcik, J. Solution conformational study of nociceptin and its 1−13 and 1−11 fragments using circular dichroism and two-dimensional NMR in conjunction with theoretical conformational analysis. *J. Pept. Sci.* **2004**, *10*, 678–690.

(37) (a) Tyndall, J. D. A.; Pfeiffer, B.; Abbenante, G.; Fairlie, D. P. Over 100 peptide-activated G protein-coupled receptors recognize ligands with turn structure. *Chem. Rev.* **2005**, *105*, 793–826. (b) Ruiz-Gómez, G.; Tyndall, J. D. A.; Pfeiffer, B.; Abbenante, G.; Fairlie, D. P. Update 1 of: Over 100 peptide-activated G protein-coupled receptors recognize ligands with turn structure. *Chem. Rev.* **2010**, *110*, PR1–PR41.

(38) Connor, M.; Yeo, A.; Henderson, G. The effect of nociceptin on Ca^{2+} channel current and intracellular Ca^{2+} in the SH-SY5Y human neuroblastoma cell line. *Br. J. Pharmacol.* **1996**, *118*, 205–207.

(39) Wang, W.; Cui, Q.; Li, Y.; Li, B.; Yang, X.; Cui, L.; Jin, H.; Qu, L. The role of ERK-1/2 in the N/OFQ-induced inhibition of delayed rectifierpotassium currents. *Biochem. Biophys. Res. Commun.* **2010**, *394*, 1058–1062.

(40) Guerrini, R.; Caló, G.; Lambert, D. G.; Carrá, G.; Arduin, M.; Barnes, T. A.; McDonald, J.; Rizzi, D.; Trapella, C.; Marzola, E.; Rowbotham, D. J.; Regoli, D.; Salvadori, S. N- and C-terminal modifications of nociceptin/orphanin FQ generate highly potent NOP receptor ligands. *J. Med. Chem.* **2005**, *48*, 1421–1427.

(41) Calo, G.; Guerrini, R.; Rizzi, A.; Salvadori, S.; Burmeister, M.; Kapusta, D. R.; Lambert, D. G.; Regoli, D. UFP-101, a peptide antagonist selective for the nociceptin/orphanin FQ receptor. *CNS Drug Rev*. **2005**, *11*, 97–112.
(42) Lapalu, S.; Moisand, C.; Butour, J. L.; Mollereau, C.; Meunier, J. C. Different domains of the ORL1 and kappa-opioid receptors are involved in recognition of nociceptin and dynorphin A. *FEBS Lett*. **1998**, *427*, 296–300.
(43) Topham, C. M.; Moulédous, L.; Poda, G.; Maigret, B.; Meunier, J. C. Molecular modelling of the ORL1 receptor and its complex with nociceptin. *Protein Eng*. **1998**, *11*, 1163–1179.
(44) Guerrini, R.; Caló, G.; Bigoni, R.; Rizzi, A.; Varani, K.; Toth, G.; Gessi, S.; Hashiba, E.; Hashimoto, Y.; Lambert, D. G.; Borea, P. A.; Tomatis, R.; Salvadori, S.; Regoli, D. Further studies on nociceptin-related peptides: discovery of a new chemical template with antagonist activity on the nociceptin receptor. *J. Med. Chem*. **2000**, *43*, 2805–2813.
(45) Fairlie, D. P.; West, M. W.; Wong, A. K. Towards protein surface mimetics. *Curr. Med. Chem*. **1998**, *5*, 29–62.
(46) Wider, G.; Dreier, L. Measuring protein concentrations by NMR spectroscopy. *J. Am. Chem. Soc*. **2006**, *128*, 2571–2576.
(47) Liu, M.; Mao, X.-a.; Ye, C.; Huang, H.; Nicholson, J. K.; Lindon, J. C. Improved WATERGATE pulse sequences for solvent suppression in NMR spectroscopy. *J. Magn. Reson*. **1998**, *132*, 125–129.
(48) Brunger, A. T. *Xplor 3.851*; Yale University: New Haven, CT, 1992.